AURORAL DYNAMICS IN THE POLAR CAP REGION

Kazuo Makita[1], Masaru Ayukawa[2], Hisao Yamagishi[2],
Masaki Ejiri[2] and Takeshi Sakanoi[3]

[1]*Takushoku University, 815-1, Tatemachi, Hachioji-shi, Tokyo 193*
[2]*National Institute of Polar Research, 9-10, Kaga 1-chome, Itabashi-ku, Tokyo 173*
[3]*Tohoku University, Aoba Aramaki, Aoba-ku, Sendai 980-77*

Abstract: The characteristics of extremely high latitude auroras are examined by using Greenland auroral data. In this paper, two different auroras obtained in the dayside and the morning sector are mainly analyzed; (1) polar arc: this aurora is observed during quiet conditions and is related to less than 100 eV precipitating electrons, and (2) polar corona: this aurora is observed during disturbed conditions and is related to a few hundred eV electrons. These two auroras may have different sources; the polar arc corresponds to the plasma mantle or low latitude boundary layer and the polar corona corresponds to the low latitude boundary layer or boundary plasma sheet. The relationships of IMF fluctuations are also examined and found that auroral enhancement and/or movement are seen in association with southward turning of the IMF.

1. Introduction

Entry of magnetosheath particles into the extremely high latitude region is strongly affected by the solar wind and also IMF conditions. Recently, several researchers reported that there are different kinds of particles near the dayside magnetospheric boundary (Rosenbauer *et al.*, 1975; Bavassano-Cattaneo and Formisano, 1978; Formisano, 1980; Johnstone, 1985). Haerendel *et al.* (1978) examined the magnetic configuration model near the magnetopause and neutral points. They show that the dayside boundary layer is located on closed field lines at lower latitude than the open entry layer and cusp field lines. They noticed that the dayside boundary layer is largely the same as the boundary layer on the nightside, seen between the plasma sheet and the tail lobe. On the other hand, low energy particles are also precipitating on the higher latitude side of the entry layer (cusp region) and in the deep polar cap.

Most recently, Newell and Meng (1992, 1994) examined precipitating particles obtained by DMSP satellite and showed the source region of the precipitating particles observed in the low altitude region. According to their results, electrons from the low latitude boundary layer are distributed between 76 and 78 degrees magnetic latitude in the dayside sector (09–15 MLT). The cusp particles are seen between 77 and 78 degrees magnetic latitude in the narrow dayside sector (11–15 MLT). The mantle particles are precipitating between 78 and 81 degrees in the dayside sector (09–15 MLT). They also show that the locations of these regions

depend on the IMF orientation and solar wind pressure.

Those precipitating particles must excite various kind of auroras in the dayside polar cusp and polar cap region. From the recent Viking auroral imager observations, ELPHINSTONE *et al.* (1993) examined the morphologies of the dayside aurora and showed the variety of auroral forms related to different magnetospheric phenomena. On the other hand, SANDHOLT *et al.* (1992) examined the auroral structure in the dayside cusp region using ground based auroral observations. Although many researchers study the cusp/cap auroras and their related phenomena, much remains unknown about the global high latitude auroral phenomena and their relationships to the particle precipitations and other phenomena obtained by satellite. In this paper, we examined the high latitude aurora obtained at Godhavn (76° MLAT) and Upernavik (80° MLAT) in Greenland in order to clarify the characteristics of high latitude auroras and their IMF dependences.

2. Characteristics of Typical High Latitude Aurora

There are several kinds of high latitude auroras from their characteristic patterns and particle precipitations. On the basis of high latitude auroras obtained at Godhavn and Upernavik, Greenland from December 1988 to January 1993, we categorized three types of high latitude aurora and examined their characteristics. They are polar arc, polar corona and discrete aurora. It is noted that there are several other kind of auroras in the high latitude region, however, the occurrence frequency of such auroras are not high, so we mainly examine the above three auroras in this paper.

Typical auroral image data are shown in Fig. 1. The left panel illustrates polar arc features. Generally, the polar arc extends from east to west and is observed frequently in the dawn and dusk sectors. This arc is stable and develops from the dayside region. The duration time of this arc is within a few minutes, it disappears
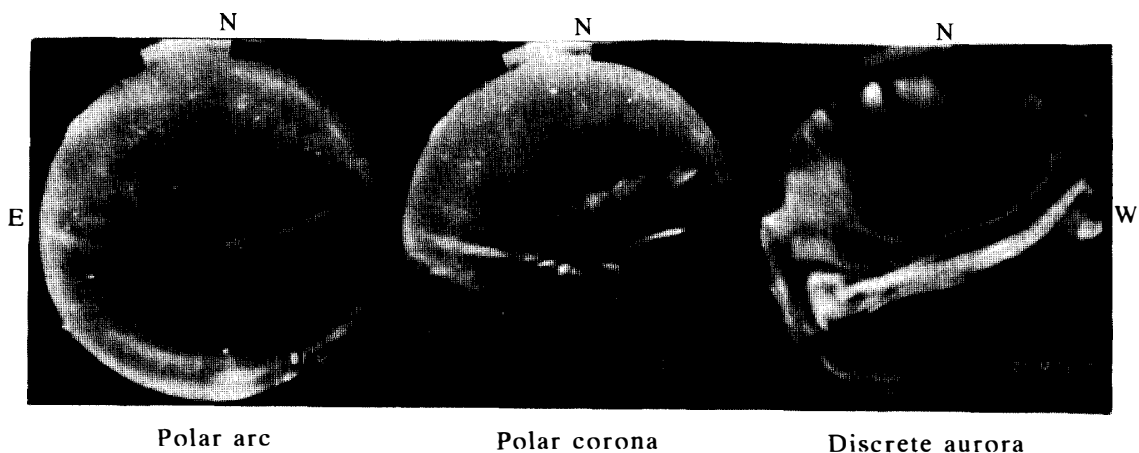

Polar arc   Polar corona   Discrete aurora

Fig. 1. *Auroral image data obtained by all-sky TV camera at Godhavn. The left panel shows polar arc observed in the dawn sector. The middle panel shows the polar corona observed in the pre-noon sector. The right panel shows the discrete aurora observed in the midnight.*

without remarkable activity. The intensity of the polar arc is very weak and less than a few kR at 557.7 nm. This arc appears during the geomagnetic quiet condition and thus may correspond to the northward IMF period. The polar arc defined here must be the same as the sun-aligned arc reported by DAVIS (1960). However, this arc does not always appear along the sun-aligned direction, especially on the dayside, so here we call it the polar arc instead of a sun-aligned arc. It is also noted that this polar arc is different from high latitude arcs and also transpolar arcs originated from the plasma sheet. According to OBARA *et al.* (1993) and others, the electron energy related to such a high latitude arc is much higher, its peak energy is > 1 keV and temperature > 200 eV. The distinct difference between a polar arc and high latitude arc is the appearance regions. Generally, a polar arc appears from the dayside region. On the contrary, a high latitude arc appears from the night side region.

The middle panel illustrates the polar corona. The polar corona is mainly observed in the dayside and morning sectors. This corona is active and continuously observed more than a few tens of minutes during the disturbed period. The corona shows ray structures within a small area and its luminosity is more than a few kR at 557.7 nm. It is found that the polar corona is more frequently observed at Godhavn than at Upernavik (this result will be reported in a separated paper), which suggests that polar corona occurrence is mainly confined to latitude less than $80°$ MLAT.

The polar corona defined here seems to be similar to the discrete patchy aurora reported by MENG and LUNDIN (1986). On the other hand, WEBER *et al.* (1986) observed the polar cap F layer patch in the extremely high latitude region. These patches were flowing from the center of the polar cap to the poleward edge of the auroral oval. The 630.0 nm airglow emission within patches is less than 500 Rayleighs. At the present, it is not clear whether the polar corona has any relationship to these F layer patches or not.

The right panel illustrates the discrete aurora near the night side region. The active discrete aurora appears during the disturbed condition and its luminosity is higher than ten kR. The characteristics of this aurora are similar to those of the oval aurora, thus, its origin is a plasma sheet which expanded poleward during the substorm.

We mainly examined the characteristics of the morning and dayside high latitude aurora, namely polar arc and polar corona. The relationship between the two kinds of auroras and geomagnetic disturbances were examined for all aurora data obtained at Godhavn, Greenland from 06 to 10 magnetic local time (MLT) December 22, 1989 to January 31, 1990. Among the above 21 days, the polar arc and polar corona events are selected, respectively. It is noted that polar arc and polar corona are sometimes observed simultaneously from 06 to 10 MLT. We selected pure polar arcs or polar coronas without mixing the two phenomena. Figure 2 illustrates the occurrence frequency of polar arcs and polar coronas as a function of Kp value. The top panel shows the dependence on Kp for 21 days including both polar arc and polar corona phenomena, where the Kp values are scatterred between 0 and 5 in all these data. The middle panel shows the distribution of Kp values for the polar arc phenomena. This suggests that the polar arc appears
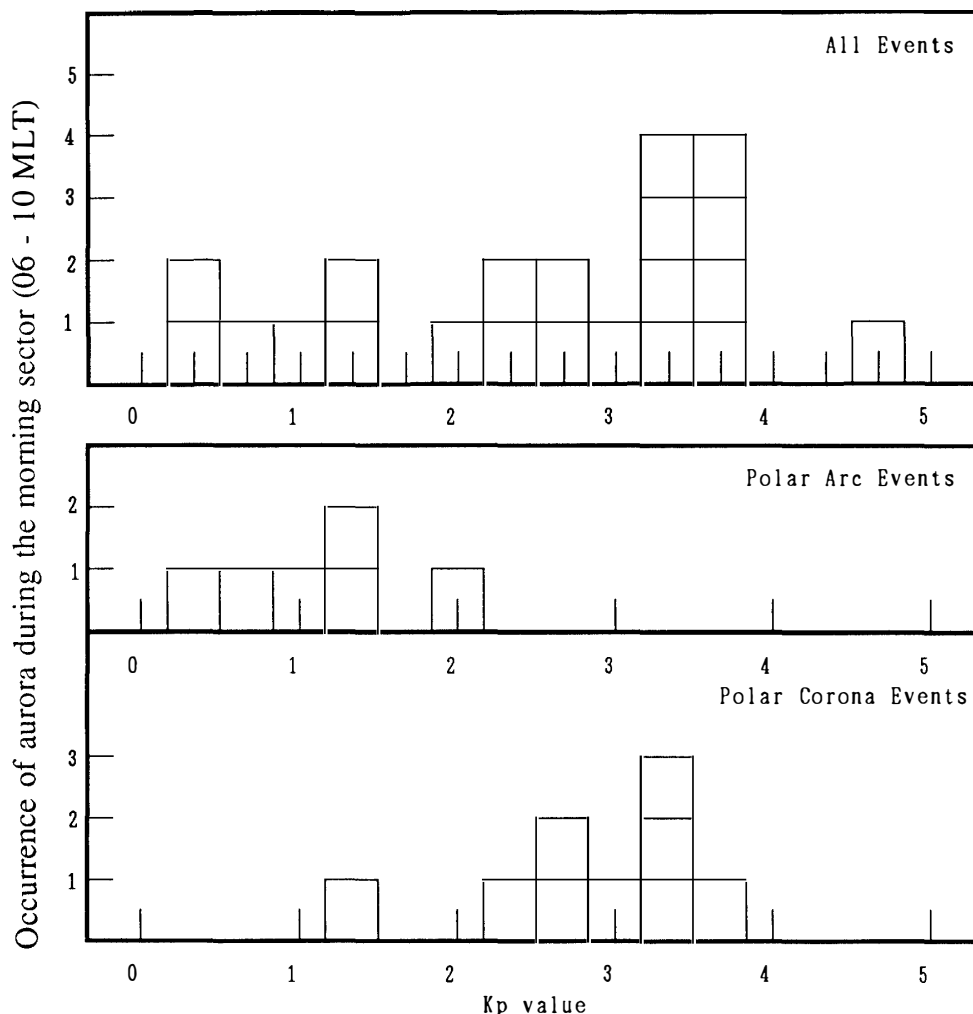
Fig. 2. The occurence frequency of polar arcs and polar coronas as a function of Kp values.
Polar arc appears during quiet period (low Kp values) and polar arc appears during
the active period (large Kp values).

during the low *Kp* values. On the other hand, the bottom panel shows the
distribution of *Kp* values for polar coronas. The polar corona appears during
moderate disturbed conditions. Although the number of selected events is not
sufficient, these results suggest that the polar arc appears during quiet periods and
polar corona appears during moderate disturbed conditions.

In order to examine the characteristics of particle precipitation for polar arcs
and polar coronas taken at Godhavn, we analyzed the simultaneous particle
precipitation data obtained by DMSP F9 satellite. Figure 3 shows the electron
differential spectrum corresponding to the polar arc and the polar corona. The left
panel shows the TV image of the polar corona and the simultaneous differential
electron spectrum observed at 1127:33 UT. In the left bottom panel, the typical
polar corona is shown when a DMSP satellite passes near the observation site. The
simultaneous electron spectrum is illustrated in the left top panel. The spectrum is
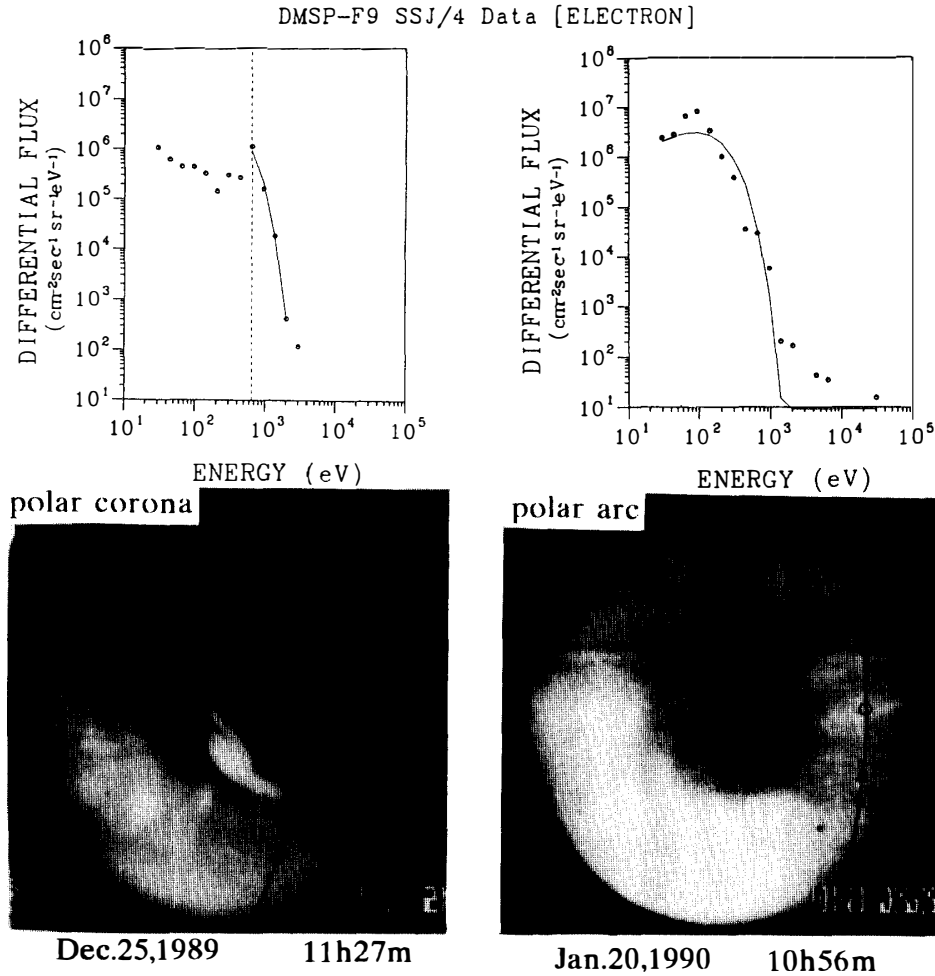fitted to the Maxwellian distribution and gives peak electron energy 646 eV, temper-

Fig. 3.   The electron and proton spectrum corresponding to the polar arcs and polar coronas. The left panel shows the electron differential spectrum for the polar corona, the peak electron energy is about 600 eV.   The right panel shows the electron differential spectrum for the polar arc, the peak electron energy is about 100 eV.   The satellite pass through near the zenith of Godhavn.   The line in the all-sky image shows the satellite orbit and the circle indicates the satellite position where the electron spectrum was obtained.

Table 1.   Characteristics of particle precipitation for polar corona and polar arc events.   The precipitating electron and ion energy corresponding to polar corona is generally much higher than that for polar arc.   The number density of electrons corresponding to polar corona is slightly lower than that for polar arc.

Aurora type	Electron			Ion
	Peak energy	Temperature	Density	Peak energy
Polar corona	≥ 100 eV	≥ 100 eV	$10^5 \sim 10^6$ (0.1/cm^3)	≥ 1 keV
Polar arc	≤ 100 eV	≤ 100 eV	$10^6 \sim 10^7$ (a few/cm^3)	≤ 1 keV

ature 156.7 eV and peak number flux $10/cm^2$ s sr eV. In the right bottom panel, the typical polar arc image is shown when a DMSP satellite passes through the east side of Godhavn. The simultaneous electron spectrum obtained at 1056:25 UT is shown in the right top panel. It shows the peak energy of about 100 eV and peak number flux of about $10/cm^2$ s sr eV. From the fitted Maxwellian distribution curve, the temperature is 86 eV in this case. We examined several other events and have summarized the characteristics of particle precipitation for polar arc and polar corona phenomena in Table 1. It indicates that the peak energy of electron precipitation is a few hundred eV and the temperature is higher than 100 eV for polar coronas, where for the polar arcs, the peak energy of electron is less than 100 eV and the temperature is also less than 100 eV. We also examined the ion precipitation data and found that the peak energy of ions is higher than 1 keV for a polar corona and lower than 1 keV for a polar arc.

3. High Latitude Auroral Dynamics and IMF *Bz* Variations

The increase of auroral luminosity and its movement are strongly controlled by the IMF *Bz* polarities and their variations. Figure 4 illustrates IMF data and the east-west meridian scanning graph obtained on December 30, 1989. The top panel is IMF *Bz* data obtained from 0800 to 0900 UT. It shows that *Bz* is positive from 0810 to 0828 UT, except for the negative spike seen from 0818 to 0820. It is noted that small positive *Bz* variation started at 0827 and soon after sharply changed from positive to negative values after 0828 UT. The east-west scanning graph is given at the bottom. It is noted that the weather is cloudy before 0800 UT and there is a data gap from 0815 to 0820 UT. So, here we show the auroral data from 0821 to 0851 UT. The auroral enhancement is seen at 0821. This activity may correspond to the magnetic negative spike between 0818 and 0820. The bright polar corona suddenly appeared near the east side region (dayside direction) at 0827 UT and gradually moved to the zenith at 0828 UT. This corona disappeared within a few minutes, a stable faint arc is observed at the equatorward side of Godhavn after that (this arc is not recognized in this east-west merdian scanning graph). It is noted that the enhancement of the polar corona at Godhavn is seen under the IMF *Bz* fluctuations. Namely, the auroral enhancement occurs when IMF *Bz* shows spiky positive variations and changes to negative values. Although it is not easy to determine the response time between IMF *Bz* variation and polar corona enhancement by using only one point auroral observation, it seems that the southward turning of IMF *Bz*

Fig. 4 (opposite). *IMF Bz data and the east-west meridian scanning graph obtained by all-sky TV. The polar corona appears from the east side at 0827 and it disappears within a few minutes. This interval corresponds to the time between 0827 (small positive fluctuations in Bz) and 0829 (sharply changed to negative value).*

Fig. 5 (opposite). *IMF Bz data and the north-south meridian scanning graph obtained by all-sky TV. The equatorward movement of the discrete aurora was seen in association with the southward turning of IMF at 0138.*
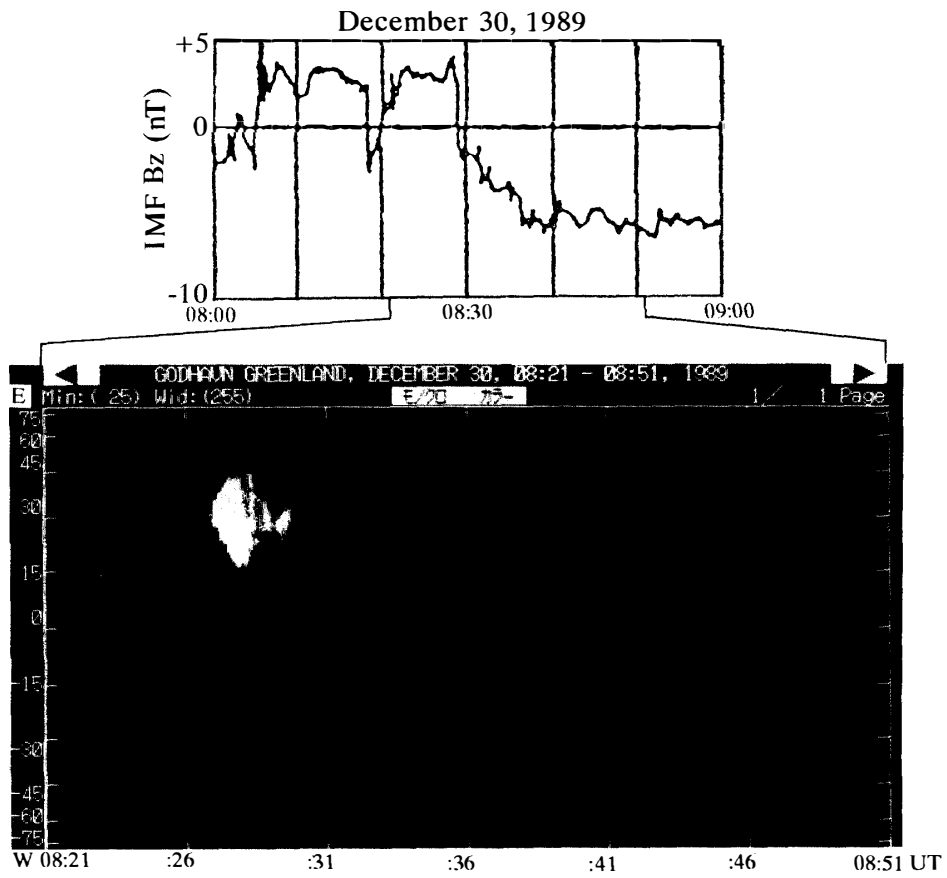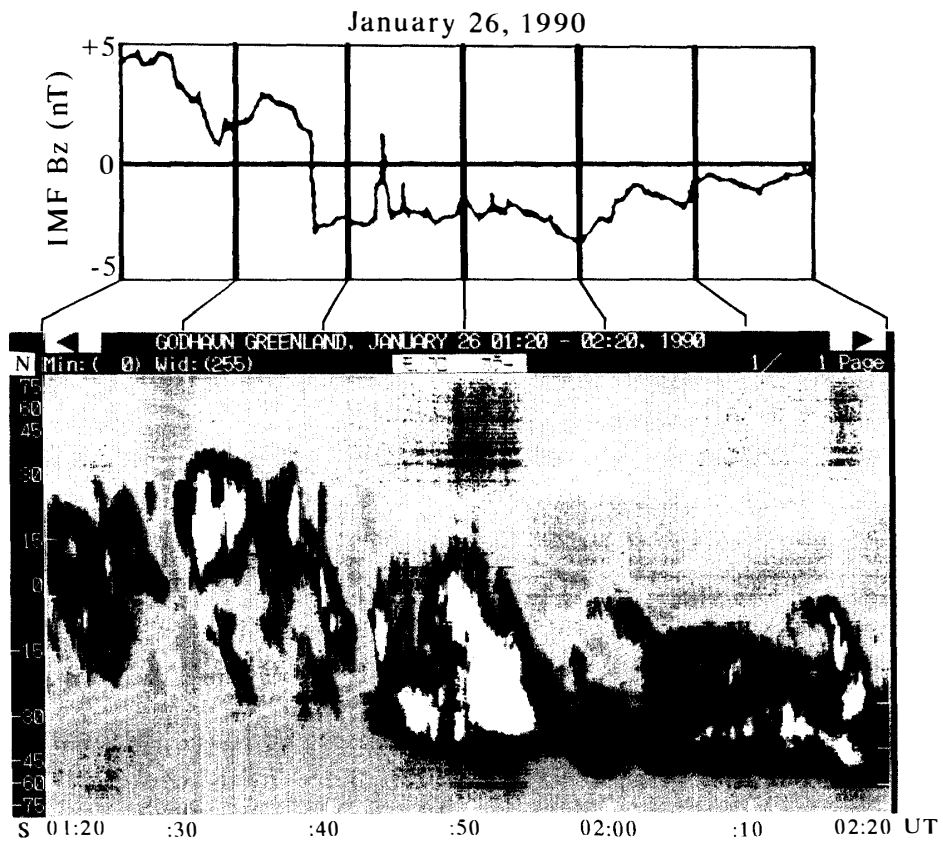
December 30, 1989

Fig. 4.

January 26, 1990

Fig. 5.

relates to the enhancement of polar corona.

Figure 5 illustrates the night side auroral movement and IMF *Bz* variations on January 26, 1990. The top panel is IMF *Bz* data from 0120 to 0220 UT. The polarity of IMF *Bz* sharply changed from positive to negative at 0136 and then remained the negative except for temporary change for a few minutes at 0143. The bottom panel illustrates the spatial variation of auroral intensity along the north to south meridian examined by all-sky TV data. The auroral movement and its intensity are seen along the magnetic north to south meridian. The discrete aurora is observed in the high latitude side of Godhavn from 0120 to 0138 UT. IMF *Bz* polarity is positive during this interval. When IMF *Bz* changes to negative at about 0138, the active discrete aurora begins to move equatorward with fluctuation of its luminosity. After 0140, which corresponds to the southward IMF conditions, discrete auroras are continuously observed at the equatorward side of Godhavn. The present example suggests that the poleward edge of the oval aurora moves equatorward in association with the southward turning of IMF. The time difference between the IMF southward turning and the equatorward movement of the aurora seems to be within a minute in this case.

4. Summary and Discussion

On the basis of Greenland aurora TV and DMSP particle data, we examined high latitude auroras. It is found that polar arc is observed during quiet condition and its peak energy is less than 100 eV. On the other hand, polar corona is observed during moderately disturbed conditions, its peak energy is a few hundred eV. According to the results of NEWELL *et al.* (1991), the plasma mantle is observed immediately poleward of the cusp or dayside auroral oval. In the mantle region, magnetosheath-like precipitation is observed and the electron number flux are about 10 times lower than in the cusp. They also mentioned that less dramatic electron acceleration events on small scales (arc phenomena) are quite common in the mantle region. From HEOS-2 data, FORMISANO (1980) reported that magneto-sheath-like electrons are less than 100 eV, the boundary layer electrons are about 170–270 eV and the plasma sheet electrons are above 1 keV. From the above results and our examinations, the polar arc precipitation is similar to the magnetosheath particle spectrum, thus its source may be the plasma mantle or partly related to low latitude boundary layer. On the other hand, polar corona precipitation is similar to the boundary layer particle spectrum, thus, its origin may be the low latitude boundary layer or partly related to plasma sheet.

For the relationship between the dayside auroral enhancements and IMF *Bz* variations, it was found that the corona aurora was enhanced during the transit period from positive to negative values of IMF *Bz*. Since the field lines of the polar cap and cusp directly interacting with the IMF, the auroral phenomena connected to these field lines must be very intimately by connected to the IMF variations. This means that the polarity of IMF *Bz* may be predicted by using auroral observations at several points of the polar cap region. Furthermore, the auroral dynamics in the

night side sector and their relationships to IMF variations are examined. In our analysis, the poleward edge of the auroral oval shifts equatorward in association with southward turning of the IMF. It is interesting and important that IMF Bz variations also directly affect the location of the poleward edge of the oval within a few minutes' interval.

Although this is a preliminary result and more examinations must be done in order to reach a final conclusion, it seems that examinations of these high latitude auroral phenomena will give us new information about solar wind-magnetosphere coupling.

Acknowledgments

References

BAVASSANO-CATTANEO, M. B. and FORMISANO, V. (1978): Low energy electrons and protons in the magnetosphere. Planet. Space. Sci., **26**, 51–63.

DAVIS, T. N. (1960): The morphology of the polar aurora. J. Geophys. Res., **65**, 3497–3500.

ELPHINSTONE, R. D., HEARN, D. J., MURPHREE, J. S., COGGER, L. L., JOHNSON, M. L. and VO, H. B. (1993): Some UV day side auroral morphologies. Auroral Plasma Dynamics, ed by R. L. LYSAK. Washington, D.C, Am. Geophys. Union, 31–45 (Geophysical Monograph 80).

FORMISANO, V. (1980): Heos 2 observations of the boundary layer from the magnetosphere to the ionosphere. Planet. Space. Sci., **28**, 245–257.

HAERENDEL, G., PASCHMANN, G., SCKOPKE, N., ROSENBAUER, H. and HEDGECOCK, P. C. (1978): The frontside boundary layer of the magnetosphere and the problem of reconnection. J. Geophys. Res., **83**, 3195–3216.

JOHNSTONE, A. D. (1985): Electron injection in the polar cusp. The Polar Cusp, ed. by J. A. HOLTET and A. EGELAND. Dordrecht, D. Reidel, 47–65.

MENG, C.-I. and LUNDIN, R. (1986): Auroral morphology of the midday oval. J. Geophys. Res., **91**, 1572–1784.

NEWELL, P. T. and MENG, C.-I. (1992): Mapping the day side ionosohere to the magnetosphere according to particle precipitation characteristics. Geophys. Res. Lett., **19**, 609–612.

NEWELL, P. T. and MENG, C.-I. (1994): Ionospheric projections of magnetospheric regions under low and high solar wind pressure conditions. J. Geophys. Res., **99**, 273–286.

NEWELL, P. T., BURKE, W. J., MENG, C.-I., SANCHEZ, E. R. and GREENSPAN, M. (1991): Identification and observations of the plasma mantle at low altitude. J. Geophys. Res., **96**, 35–45.

OBARA, T., MUKEI, T., HAYAKAWA, H., NISHIDA, A., TSURUDA, K. and FUKUNISHI, H. (1993): Akebono (EXOS-D) observations of small-scale electromagnetic signatures relating to polar cap precipitation. J. Geophys. Res., **98**, 11153–11159.

SANDHOLT, P. E., LOCKWOOD, M., DENIG, W. F., ELPHIC, R. C. and LEONTJEV, S. (1992): Dynamical auroral structure in the vicinity of the polar cusp: Multipoint observations during southward and northward IMF. Ann. Geophys., **10**, 483–497.

ROSENBAUER, H., GRUNWALD, H., MONTOGOMERY, M. P., PASCHMAN, G. and SCKOPKE, N. (1975): Heos 2 plasma observations in the distant polar magnetosphere: The plasma mantle. J.

Geophys. Res., **80**, 2723–2737.

WEBER, E. J., KLOBUCHAR, J. A., BUCHAU, J. and CARLSON, H. C., Jr. (1986): Polar cap *F* layer patches: Structure and dynamics. J. Geophys. Res., **91**, 12121–12129.